

We are IntechOpen, the world's leading publisher of Open Access books Built by scientists, for scientists

6,900

Open access books available

186,000

International authors and editors

200M

Downloads

Our authors are among the

154

Countries delivered to

TOP 1%

most cited scientists

12.2%

Contributors from top 500 universities



WEB OF SCIENCE™

Selection of our books indexed in the Book Citation Index
in Web of Science™ Core Collection (BKCI)

Interested in publishing with us?
Contact book.department@intechopen.com

Numbers displayed above are based on latest data collected.
For more information visit www.intechopen.com



Helical Antennas in Satellite Radio Channel

Maja Škiljo and Zoran Blažević
*University of Split, Faculty of electrical engineering,
mechanical engineering and naval architecture,
Croatia*

1. Introduction

Monofilar and multifilar helical antennas are the most widely proposed antennas in satellite communications systems. The main reason why these antennas constitute an asset in applications concerning satellite and space communications generally is circular polarization. Good axial ratio provides precise measurement of the polarization of the received signal due to immunity of the circularly polarized wave to Faraday rotation of the signal propagating through the ionosphere.

In addition to circular polarization, monofilar helical antennas offer the advantage of high gain in axial direction over a wide range of frequencies which makes them suitable for applications in broadband satellite communications. Split beam and conical beam radiation patterns of bifilar and quadrifilar helical antennas respectively, offer even more applications in mobile satellite communications (Kilgus, 1975; Nakano et al., 1991). Also, backfire helical antenna has stood out as a better feed element for parabolic reflector than the axial mode helical antenna and horn antennas (Nakano et al., 1988). Beside the number of wires in helical antenna structure, it is possible to use antenna's physical parameters to control the directivity pattern. Phase velocity of the current can be controlled by changing the pitch angle and circumference (Kraus, 1988; Mimaki & Nakano, 1998), and the ground plane can be varied in its size and shape to achieve a certain form of radiation pattern and higher antenna gain (Djordjevic et al., 2006; Nakano et al., 1988; Olcan et al., 2006). Various materials used in helical antenna design, even only for the purpose of mechanical support or isolation, can noticeably influence the antenna's performance so this should be taken into account when designing and modeling the desirable helical antenna structure (Casey & Basal, 1988a; Casey & Basal, 1988b; Hui et al., 1997; Neureuther et al., 1967; Shestopalov et al., 1961; Vaughan & Andersen, 1985).

A theoretical study of a sheath, tape and wire helix given in (Sensiper, 1951) provided the base for a physical model of the helical antenna radiation mechanism. The complex solutions of the determinantal equation for the propagation constants of the surface waves traversing a finite tape helix are used to calculate the current distribution on helical antenna in (Klock, 1963). The understanding of the waves propagating on the helical antenna structure can also provide a good assessment of the circular polarization purity as well as the estimation of varying the helical antenna radiation characteristics by changing the antenna's physical parameters and using various materials in helical antenna design (Maclean & Kouyoumjian, 1959; Neureuther et al., 1967; Vaughan & Andersen, 1985).

Although an analytical approach can sometimes provide a fast approximation of helix radiation properties (Maclean & Kouyoumjian, 1959), generally it is a very complicated procedure for an engineer to apply efficiently and promptly to the specified helical antenna design. Therefore, we combine the analytical with the numerical approach, i. e. the thorough understanding of the wave propagation on helix structure with an efficient calculation tool, in order to obtain the best method for analyzing the helical antenna.

In this chapter, a theoretical analysis of monofilar helical antenna is given based on the tape helix model and the antenna array theory. Some methods of changing and improving the monofilar helical radiation characteristics are presented as well as the impact of dielectric materials on helical antenna radiation pattern. Additionally, backfire radiation mode formed by different sizes of a ground reflector is presented. The next part is dealing with theoretical description of bifilar and quadrifilar helices which is followed by some practical examples of these antennas and matching solutions. The chapter is concluded with the comparison of these antennas and their application in satellite communications.

2. Monofilar helical antennas

The helical antenna was invented by Kraus in 1946 whose work provided semi-empirical design formulas for input impedance, bandwidth, main beam shape, gain and axial ratio based on a large number of measurements and the antenna array theory. In addition, the approximate graphical solution in (Maclean & Kouyoumjian, 1959) offers a rough but also a fast estimation of helical antenna bandwidth in axial radiation mode. The conclusions in (Djordjevic et al., 2006) established optimum parameters for helical antenna design and revealed the influence of the wire radius on antenna radiation properties. The optimization of a helical antenna design was accomplished by a great number of computations of various antenna parameters providing straightforward rules for a simple helical antenna design.

Except for the conventional design, the monofilar helical antenna offers many various modifications governed by geometry (Adekola et al., 2009; Kraft & Monich, 1990; Nakano et al., 1986; Wong & King, 1979), the size and shape of reflector (Carver, 1967; Djordjevic et al., 2006; Nakano et al., 1988; Olcan et al., 2006), the shape of windings (Barts & Stutzman, 1997, Safavi-Naeini & Ramahi, 2008), the various guiding (and supporting) structures added (Casey & Basal, 1988a; Casey & Basal, 1988b; Hui et al., 1997; Neureuther et al., 1967; Shestopalov et al., 1961; Vaughan & Andersen, 1985) and other. This variety of multiple possibilities to slightly modify the basic design and still obtain a helical antenna performance of great radiation properties with numerous applications is the motivation behind the great number of helical antenna studies worldwide.

2.1 Helix as an antenna array

A simple helical antenna configuration, consisted of a perfectly conducting helical conductor wound around the imaginary cylinder of a radius a with some pitch angle ψ , is shown in Fig. 1. The conductor is assumed to be a flat tape of an infinitesimal thickness in the radial direction and a narrow width δ in the azimuthally direction. The antenna geometry is described with the following parameters: circumference of helix $C = \pi D$, spacing p between the successive turns, diameter of helix $D = 2a$, pitch angle $\psi = \tan^{-1}(p/\pi D)$, number of turns N , total length of the antenna $L = Np$, total length of the wire $L_n = NL_0$ where L_0 is the wire length of one turn $L_0 = (C^2 + p^2)^{1/2}$.

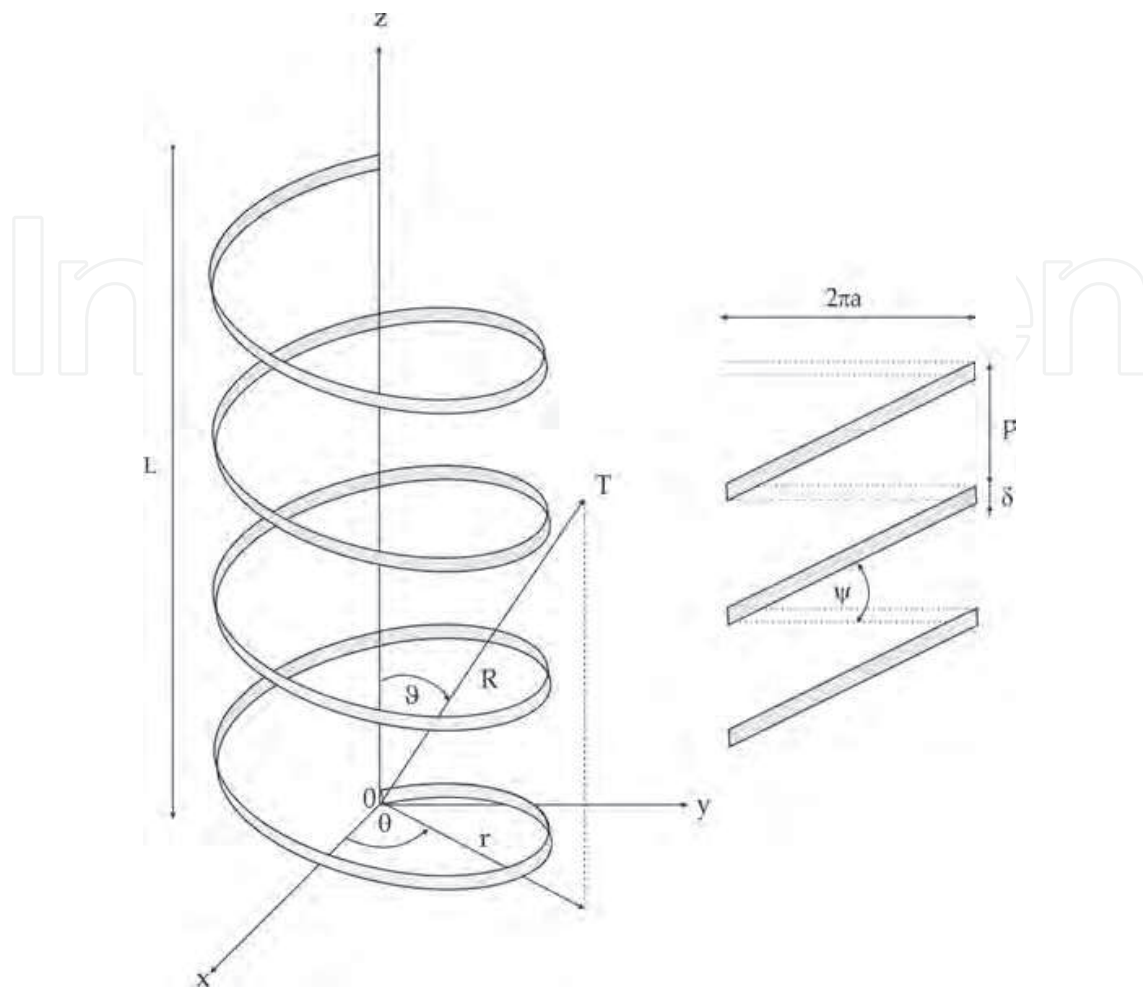


Fig. 1. The tape helix configuration and the developed helix.

Considering the tape is narrow, $\delta \ll \lambda, p, a$, assuming the existence of electric and magnetic currents in the direction of the antenna axis of symmetry and applying the boundary conditions on the surface of the helix, we can derive the field expressions for each existing free mode as the total of an infinite number of space harmonics caused by helix periodicity with the propagation constants $h_m = h + 2\pi m/p$, where m is an integer (Sensiper, 1951). Knowing the field components at the antenna surface, the far field in spherical coordinates (R, θ, ϑ) for each existing mode can be obtained upon by the Kirchhoff-Huygens method. The contribution to the radiated field of each space harmonic can be written in the form of the element factor and the array factor product, thus the total radiated electric field caused by the particular mode is expressed as (Cha, 1972; Kraus, 1948; Shestopalov, 1961; Vaughan & Andersen, 1985):

$$E_\theta(\theta, \vartheta) = \sum_{m=-\infty}^{\infty} F_{\theta m}(\theta, \vartheta) G_m(\vartheta; L), \quad (1)$$

$$E_\vartheta(\theta, \vartheta) = \sum_{m=-\infty}^{+\infty} F_{\vartheta m}(\theta, \vartheta) G_m(\vartheta; L). \quad (2)$$

The element factors $F_{\theta m}$ and $F_{\vartheta m}$ represent the contribution of each turn to the total field in some far point of the space due to the m^{th} cylindrical space harmonic, and are determined as:

$$F_{\theta m}(\theta, \vartheta) = 2 \left(\frac{m}{ka} E_{zm}^a \cot \vartheta - E_{\theta m}^a \sin \vartheta \right) J_m - jZ_0 H_{zm}^a (J_{m+1} - J_{m-1}), \quad (3)$$

$$F_{\vartheta m}(\theta, \vartheta) = 2Z_0 \left(\frac{m}{ka} H_{zm}^a \cot \vartheta - H_{\theta m}^a \sin \vartheta \right) J_m + jE_{zm}^a (J_{m+1} - J_{m-1}), \quad (4)$$

where $E_{\theta m}^a$, $E_{\vartheta m}^a$, and $H_{\theta m}^a$, $H_{\vartheta m}^a$ are the m^{th} cylindrical space harmonic amplitudes of electric and magnetic field spherical components at the antenna surface respectively, $k = 2\pi f \sqrt{\mu_0 \epsilon_0} = 2\pi f/c$ is the free-space wave-number, $Z_0 = \sqrt{\mu_0/\epsilon_0} = 120\pi \Omega$ is the impedance of the free space, and $J_m = J_m(ka \sin \vartheta)$ is the ordinary Bessel function of the first kind and order m . The complex array factor G_m is calculated for each space harmonic as:

$$G_m(\vartheta; L) = L \text{sinc}(N \Phi_m/2) e^{jN \Phi_m/2}, \quad (5)$$

where Φ_m is the phase difference for the m^{th} harmonic between the successive turns:

$$\Phi_m = kL \left(\cos \vartheta - \frac{h_m}{k} \right). \quad (6)$$

Unlike the element factor, the array factor defines the directivity and does not influence the polarization properties of the antenna. It is found (Kraus, 1949) that, although (3) and (4) are different in form, the patterns (1) and (2) for entire helix are nearly the same, and the similar could also be stated for the dielectrically loaded antenna. Furthermore, the main lobes of E_θ and E_ϑ patterns are very similar to the array factor pattern. Hence, the calculation of the array factor alone suffices for estimations of the antenna properties at least for long helices.

Assuming only a single travelling wave on the helical conductor, following (1)-(2), a helix antenna can be depicted as an array of isotropic point sources separated by the distance p , as in Fig. 2. The normalized array factor is:

$$G_A = \frac{\sin(N \Phi/2)}{N \sin(\Phi/2)}. \quad (7)$$

This is justified as the absolute of (5) and (7) are approximately equal, and small differences become noticeable only for $N \leq 5$. Denoting the phase difference for the fundamental space harmonic of axial mode as $\Phi_0 = \Phi$ in (6), the Hansen-Woodyard condition for the maximum directivity in the axial direction ($\vartheta = 0$) states that (Maclean & Kouyoumjian, 1959):

$$\Phi = -2\pi \left(1 + \frac{1}{2N} \right), \quad (8)$$

Ideally, applying (6)-(8), the radiation characteristics of the helical antenna and the antenna geometry can be directly connected by single variable, the velocity v of the surface wave (Kraus, 1949; Maclean & Kouyoumjian, 1959; Nakano et al., 1986; Wong & King, 1979). As the wave velocities in a finite helix are hard to calculate, those calculated for the infinite

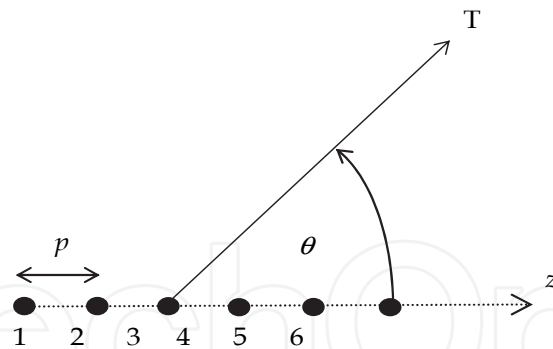


Fig. 2. The array of N point sources.

helix can be applied as a fair approximation. The determinantal equation for the wave propagation constants on an infinite helical waveguide is given and analyzed in (Klock, 1963; Mitra, 1963; Sensiper, 1951, 1955) and generalized forms of the equation for helices filled with dielectrics are considered in (Blazevic & Skiljo, 2010; Shestopalov et al. 1961; Vaughan & Andersen, 1985). The solutions are obtained in a form of the Brillouin diagram for periodic structures, which dispersion curves are symmetrical with respect to the ordinate (the circumference of the helix in wavelengths). The calculated propagation constants (phase velocities) of free modes are real numbers settled within the triangles defined by lines $ka = \pm ha \mp |m| \cot \psi$, among which those with $|m| = 1$ comply with the condition (8) for infinite arrays. The $m = 0$ and $m = -1$ regions of the diagram refer to the so called normal and the axial mode, respectively. The Brillouin diagram provide the information about the group velocity of the surface waves calculated as the slope of the dispersion curves at given frequency. It is important to note that the phase and group velocities on the helix may have opposite directions. When the circumference of the helix is small compared to the wavelength, the normal mode dominates over the others and the maximum radiated field is perpendicular to helix axis. These electric field components are then out of phase so the total far field is usually elliptically polarized. Due to the narrow bandwidth of radiation, the normal mode helical antenna is limited to narrow band applications (Kraus, 1988). Axial radiation mode is obtained when the circumference of helix is approximately one wavelength, achieving a constructive interference of waves from the opposite sides of turns and creating the maximum radiation along the axis. Helical antenna in the axial mode of radiation is a circularly polarized travelling-wave wideband antenna.

However, due to the assumption of the existence of only a single travelling wave, the modeling of helical antenna as a finite length section of the helical waveguide has some practical shortcomings, which becomes more problematical as the antenna length becomes shorter. Consider an example of the typical axial mode current distribution on Fig. 3, obtained at $C_\lambda = 1.0$ for the helical antenna with $\psi = 14^\circ$ and $N = 12$. We may observe three regions: the exponential decaying region away from the source, the surface wave region after the first minimum and the standing wave due to reflection of the outgoing wave at the open antenna end. The works of (Klock, 1963; Kraus, 1948, 1949; Marsh, 1950) showed that the approximate current distribution can be estimated assuming two main current waves, one with a complex valued phase constant settled in the region of normal mode ($m = 0$) that forms a standing wave deteriorating antenna radiation pattern, and one with real phase constant in the region of the axial mode ($m = -1$) that contributes to the beam radiation.

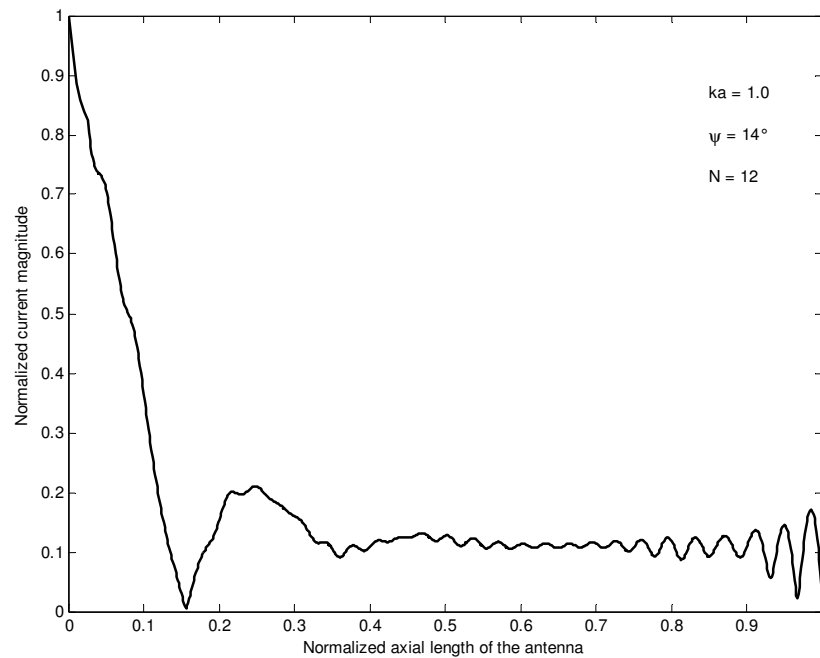


Fig. 3. A typical axial mode current distribution on helical antenna.

The analytical procedure of a satisfying accuracy for determining the relationship between the powers of the surface waves traversing the arbitrary sized helical antenna may still be sought using a variational technique, assuming the existence of only two principal propagation modes (normal and axial), and a sinusoidal current distributions for each of them taking into account the velocities calculated for the infinite helical waveguide, as shown by (Klock, 1963). However, as the formula for the total current on the helix involves integrals of a very complex form, one may rather chose to use the classical design data given in (Kraus, 1988) which, for helices longer than three turns, define the optimum design parameters in a limited span of the pitch angles in the frequency range of the axial mode. The semi-empirical formulas for antenna gain G in dB, input impedance R in ohms, half power beam-width $HPBW$ in degrees and axial ratio AR , are given by:

$$G = 11.8 + 10 \log \left(N \left(\frac{p}{\lambda} \right) \left(\frac{C}{\lambda} \right)^2 \right), \quad (9)$$

$$R = 140 \frac{C}{\lambda}, \quad (10)$$

$$AR = \frac{2N + 1}{2N}, \quad (11)$$

$$HPBW = \frac{52}{\left(\frac{C}{\lambda} \right) \sqrt{N \left(\frac{p}{\lambda} \right)}}. \quad (12)$$

Because of the traveling-wave nature of the axial-mode helical antenna, the input impedance is mainly resistive and frequency insensitive over a wide bandwidth of the antenna and can be estimated by (10). The discrepancy from a pure circular polarization, described with axial ratio AR , depends on the number of turns N and it approaches to unity as the number of turns increases. It is interesting to note that this formula is obtained by Kraus using a quasi-empirical approach where the phase velocity is assumed to always satisfy the Hansen-Woodyard condition for increased directivity. The reflected current degrades desired polarization in forward direction and by suppressing it (with tapered end for example); the formula (11) becomes more accurate (Vaughan & Andersen, 1985). However, King and Wong reported that without the end tapering the axial ratio formula often fails (Wong & King, 1982). Also, based on a great number of experimental results, they established that in the equation (13), valid for $12^\circ < \psi < 15^\circ$, $3/4 < C/\lambda < 4/3$ and $N > 3$, numerical factor can be much lower than 15, usually between 4.2 and 7.7 (Djordjevic et al., 2006), providing a different expression for the helical antenna gain:

$$G = 8.3 \left(\frac{\pi D}{\lambda_p} \right)^{\sqrt{N+2}-1} \left(\frac{Np}{\lambda_p} \right)^{0.8} \left[\frac{\tan 12.5^\circ}{\tan \psi} \right]^{\frac{\sqrt{N}}{2}}, \quad (13)$$

where λ_p is wavelength at peak gain.

The existence of multiple free modes on a helical antenna makes the theoretical analysis even more complicated when a dielectric loading is introduced. Consider two examples of the Brillouin diagram in the region $m = -1$ for the case of $\psi = 13^\circ$, $\delta = 1$ mm, $N = 10$ given on Fig. 4 a) and b) respectively. The first refers to the empty helix and the second to the helix filled uniformly with a lossless dielectric of relative permittivity $\epsilon_r = 6$. The A points mark the intersections of the dispersion curves of the determinantal equation with the line defined by the Hansen-Woodyard condition (8). Obviously, their positions depend on the number of turns. Point B marks the calculated upper frequency limit of the axial mode, f_B i.e. the frequency at which the SLL is increased to 45 % of the main beam, the criterion adopted from (Maclean & Kouyoumjian, 1959). In the case of helical antenna with dielectric core, due to the difference in permittivity of the antenna core and surrounding media, it can be noted that the solutions shape multiple branches. It can also be shown that the number of branches increases rapidly by increasing the permittivity and decreasing the pitch angle.

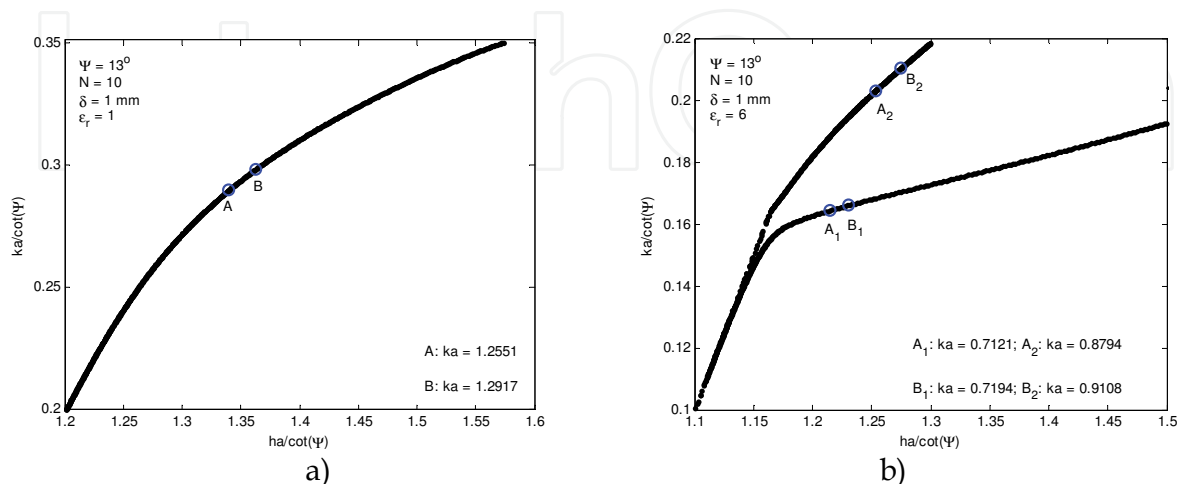


Fig. 4. A section of the Brillouin diagram in the axial mode region ($m = -1$) for the tape helix with parameters $\psi = 13^\circ$, $\delta = 1$ mm, $N = 10$, $\epsilon_r = 1$ a) and $\epsilon_r = 6$ b).

The existence of multiple axial modes as in Fig. 4 b) implicates a possibility of the existence of a number of optimal frequencies (A points), one for each axial mode. However, if the permittivity is high enough and the pitch angle low enough, the power of the lowest axial mode may be found to be insufficient to shape a significant beam radiation. Then the solution A at the lowest mode branch of the dispersion curve is settled below the minimum beam mode frequency f_L . This frequency limit marks the frequency at which the axial mode power starts to dominate over the normal mode power. It is usually determined as the lowest frequency at which the circular polarization is formed i.e. the axial ratio is less than two. Also, the HPBW of the main lobe falls below 60 degrees but this criterion can be strictly applied only for longer helices (longer than ten turns). As the working frequency starts to surmount this limit, the current magnitude distribution is transformed steadily toward the classical shape of the axial mode current (Kraus, 1988) as in Fig. 3. Also, as the classical current distribution forms, the character of the input impedance starts to be mainly real. It is found in (Maclean & Kouyoumjian, 1959) that the lower limit remains approximately constant regardless of the antenna length. This fact is confirmed for the dielectrically loaded helices as well in (Blazevic & Skiljo, 2010). It is also noted that the change in the maximum axial mode frequency with varying permittivity and pitch angle as the consequence of the change of the surface wave group velocity is much more emphasized than the change of the minimum frequency. This means that, as the optimal frequency becomes lower, the axial mode bandwidth shrinks. The overall effect of the permittivity and pitch angle on the fractional axial mode bandwidth (defined as the ratio of the bandwidth and twice the central frequency) for the various antenna lengths is depicted on Fig. 5.

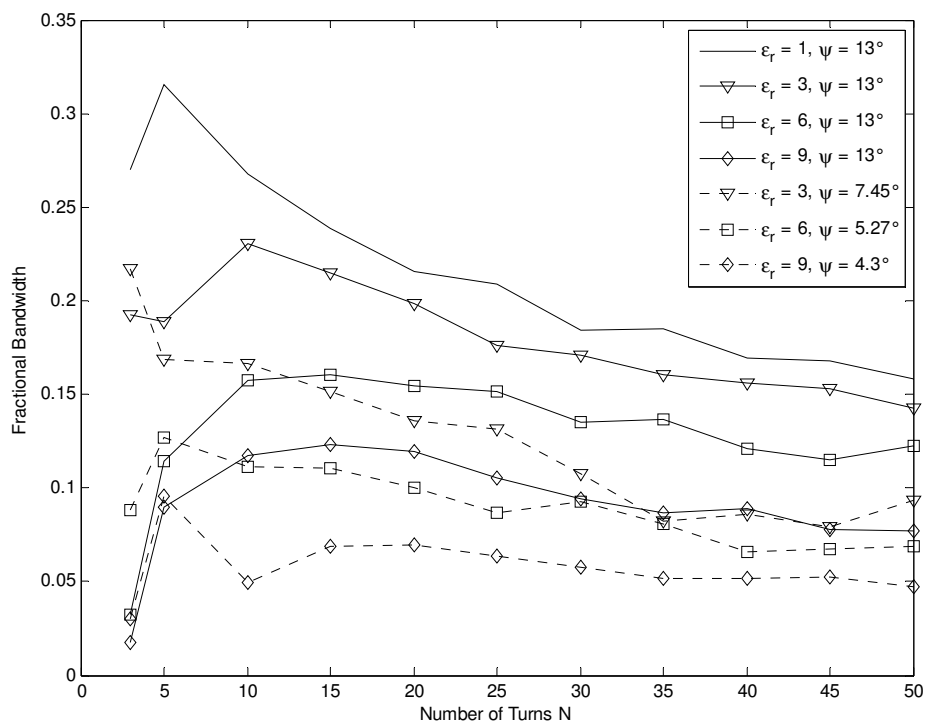


Fig. 5. The axial mode fractional bandwidth of the antennas for various dielectric loadings and pitch angles vs. number of turns.

2.2 Impact of materials used in helical antenna design

A frequently used antenna is the conventional monofilar helical structure wrapped around a hollow dielectric cylinder providing a good mechanical support, especially for thin and long helical antennas. In the case of commercially manufactured helical antennas they are often covered with non-loss dielectric material all over, while in amateur applications sometimes low cost lossy materials take place. The properties of various materials used in antenna design and their selection can be of great importance for meeting the required antenna performance, and the purpose of this chapter is to provide an insight to its influence based on a practical example.

The CST Microwave Studio was used to analyze the impact of various materials and their composition on helical antenna design and optimal performance. Since the chapter focuses on longer antennas, a 12-turn helix was chosen. We created the helical structure with the following parameters: $f = 2430$ MHz, $D = 42$ mm, $C = 132$ mm, $p = 33$ mm, $L = 396$ mm, $N = 12$, $a = 1$ mm and $\Psi = 14^\circ$. Instead of infinite ground plane commonly used in numerical simulations, we formed a round reflector with the diameter of $D_r = 17$ cm to be closer to the widespread practical design. The resistance of the source is selected to be 50Ω and the thickness of the dielectric tube in practical design is 1mm.

The antenna shown in Fig. 6 a) is the reference model of the helical antenna constructed of a perfectly conducting helical conductor and a finite size circular reflector using the hexahedral mesh.

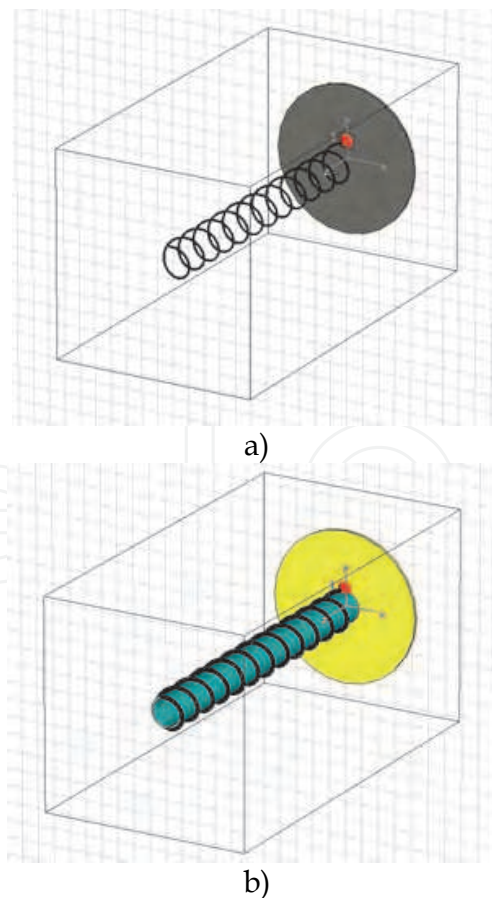


Fig. 6. The simulated helical antenna structures: a) the reference model and b) the practical design simulation.

The simulation results in Fig. 7 demonstrate the influence of applied materials on the antenna VSWR and gain in frequency band from 1.8-2.8 GHz. Each material was examined separately except for the practical design of the antenna which included all the materials used. First step to practical design of the helical antenna depicted in Fig. 6 a) was the replacement of the PEC material with the copper one, which produced negligible effects on the antenna parameters as expected. Lossy dielectric wire coating added to reference model with permittivity and conductivity selected to be $\epsilon_r = 3$ and $\sigma = 0.03$ S/m, however, caused noticeable change in the overall antenna performance. The antenna input impedance is decreased where primarily the capacitive reactance is decreased because of the higher permittivity along the helical conductor. Also, the gain is decreased and the frequency bandwidth of the antenna is shifted to somewhat lower frequencies. The empty dielectric tube (EDT), often used as a mechanical support for long antennas, is analyzed in two steps. First, non-loss EDT (with $\epsilon_r = 3$) added to the reference model, produced gain decrease and the bandwidth shift. At the same time, the antenna input impedance decreases causing the improvement of VSWR. When the conductivity of $\sigma = 0.03$ S/m is added in second step, these effects are much more emphasized, especially for the antenna gain.

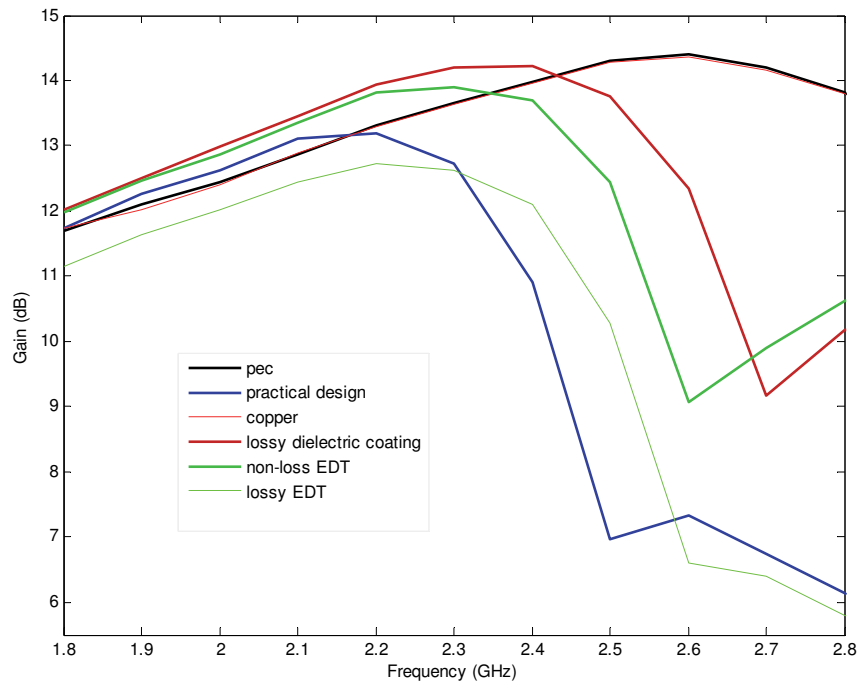
Comparing the obtained antenna gain of 13.96 dB at $f = 2.43$ GHz of reference PEC model with (9) and (13), where calculated gains are $G = 17.44$ dB and $G = 13.21$ dB respectively, it is found that the first formula is too optimistic as expected, and the second one is acceptable for some readily estimation of helical antenna gain. To the reference, the final practical antenna design, comprising the copper helical wire covered with lossy dielectric wire coating wounded around the lossy dielectric tube, and the finite size circular reflector, achieves gain of 10.91 dB at 2.43 GHz and peak gain of 13.18 dB at 2.2 GHz. Thus, in comparison with PEC helical antenna in free space, the practical antenna performance is significantly influenced by the dielectric coating and supporting EDT.

2.3 Changing the parameters of helix to achieve better radiation characteristics

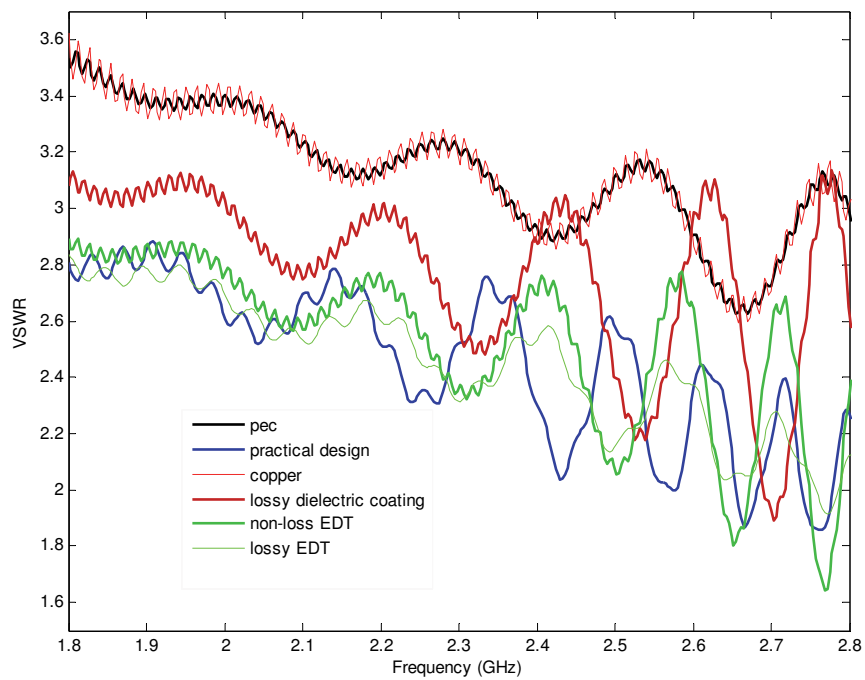
High antenna gain and good axial ratio over a broad frequency band are easily achieved by various designs of a helical antenna which can take many forms by varying the pitch angle (Mimaki and Nakano, 1998; Nakano et al., 1991; Sultan et al., 1984), the surrounding medium (Bulgakov et al., 1960; Casey and Basal, 1988; Vaughan and Andersen, 1985) and the size and shape of reflector (Djordjevic et al., 2006; Nakano et al., 1988; Olcan et al., 2006). In this chapter, we introduce a design of the helical antenna obtained by combining two methods to improve the radiation properties of this antenna; one is changing the pitch angle, i.e. combining two pitch angles (Mimaki and Nakano, 1998; Sultan et al., 1984) and the other is reshaping the round reflector into a truncated cone reflector (Djordjevic et al., 2006; Olcan et al., 2006).

It is shown (Mimaki and Nakano, 1998) that double pitch helical antenna radiates in endfire mode with slightly higher gain over wider bandwidth. Two pitch angles were investigated; 2° and 12.5° , along different lengths of the antenna. Their relative lengths were varied in order to obtain a wider bandwidth with higher antenna gain. In (Skiljo et al., 2010) the axial mode bandwidth was examined by means of parameters defining the limits of the axial radiation mode: axial ratio, HPBW, side lobe level (SLL) and total gain in axial direction, whereas the method of changing the pitch angle was applied to a helical antenna wounded around a hollow dielectric cylinder with the pitch angle of 14° . The maximum gain of the antennas with variable lengths h/H , where h is the antenna length where pitch angle $\psi_h = 2^\circ$

and H is the rest of the antenna with $\psi_H = 12.5^\circ$, is achieved with $h/H = 0.26$ (Mimaki and Nakano, 1998; Skiljo et al., 2010).



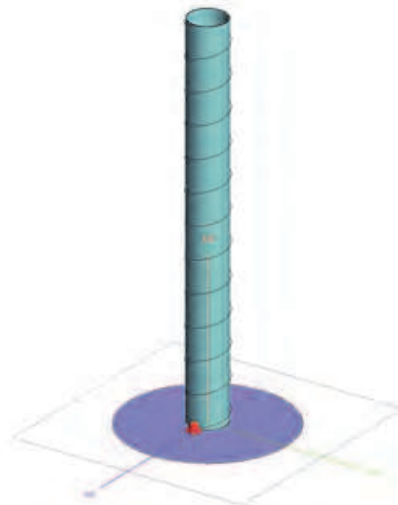
a)



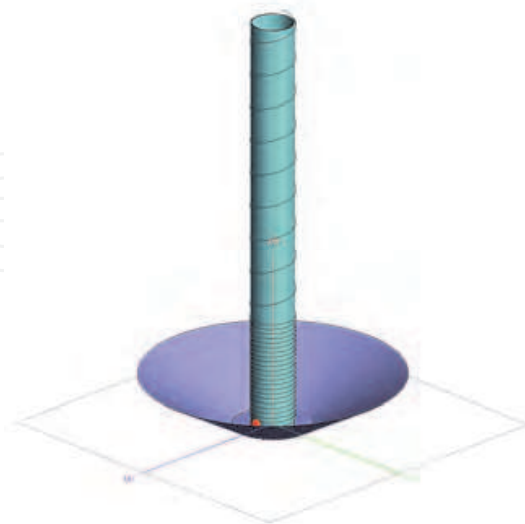
b)

Fig. 7. The simulation results of material influence on antenna a) gain and b) VSWR.

Various shapes of ground plane were considered: infinite ground plane, square conductor, cylindrical cup and truncated cone, whereas the later produced the highest gain increase relative to the infinite ground plane. So, we used the truncated cone reflector with optimal cone diameters $D_1 = 1.3\lambda$ and $D_2 = 0.4\lambda$ and height $h = 0.5\lambda$ in order to maximize the gain of the previously simulated double pitch helical antenna (Skiljo et al., 2010). Applying the criteria for the cut-off frequencies of the axial mode from chapter 2.1, it is observed that the bandwidth of the axial mode is not increased (it is slightly shifted towards lower frequencies) by using two pitch angles and a truncated cone reflector. Fig 8 a) shows the antenna model used in chapter 2.2 with non loss dielectric tube (with $\epsilon_r = 3$) and b) the simulated double pitch helical antenna.

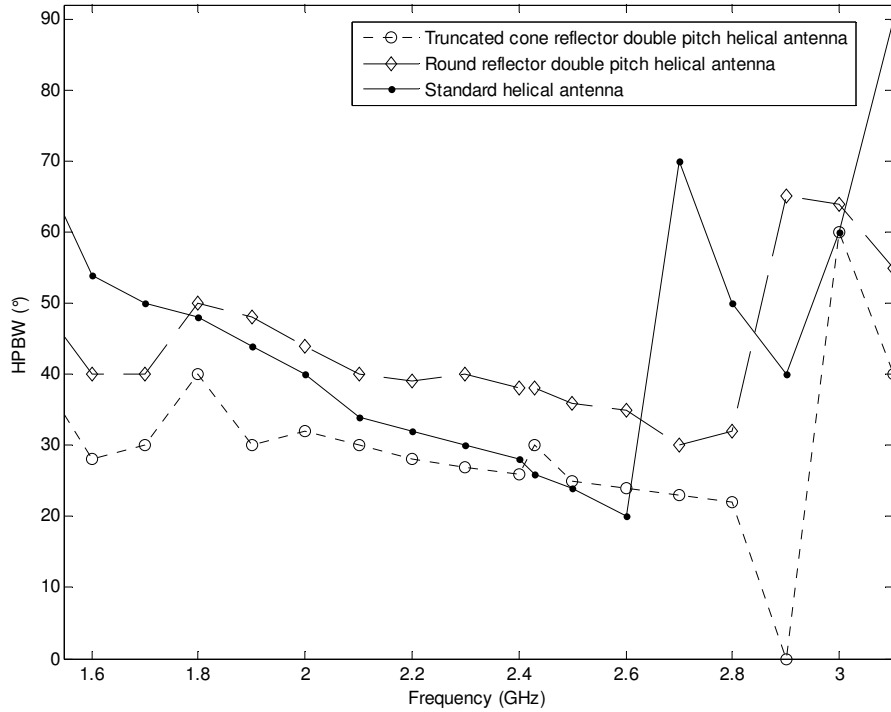


a)

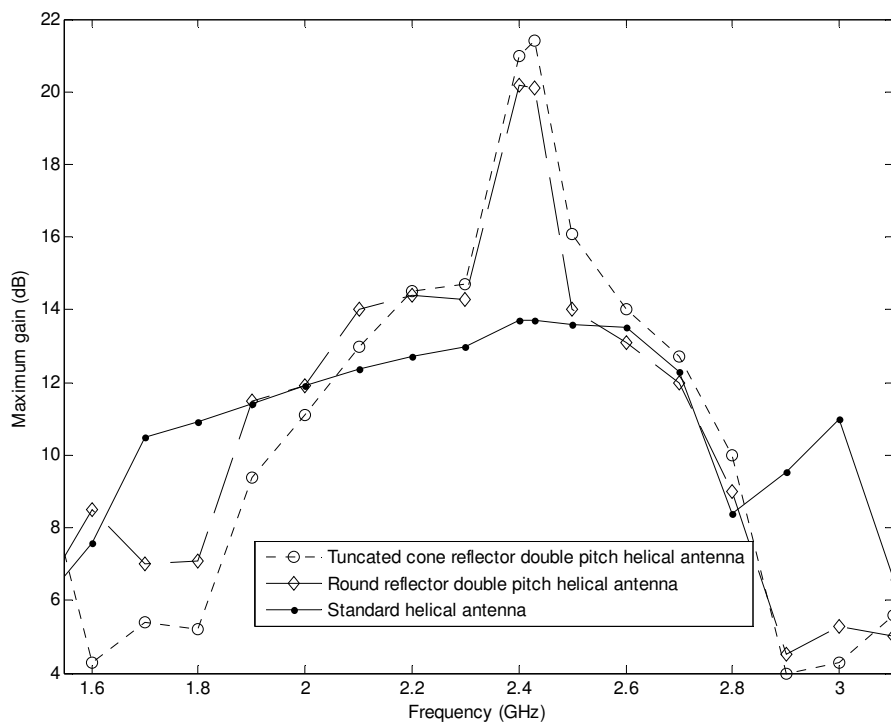


b)

Fig. 8. Simulation of the a) standard twelve turn helical antenna and b) double pitch helical antenna with truncated cone reflector.



a)



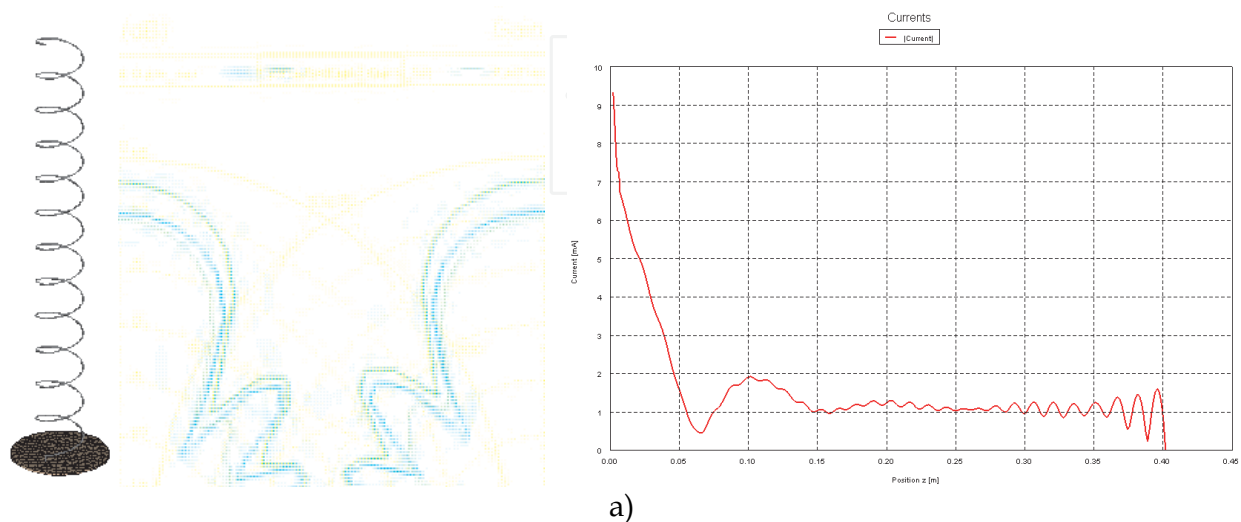
b)

Fig. 9. a) HPBW and b) total antenna gain comparison between the standard twelve turn helical antenna, double pitch helical antenna with truncated cone, and with round reflector.

The results in Fig. 9 depict that HPBW is mainly better in case of the truncated cone reflector but worse with the round reflector, and the antenna gain is improved when using the truncated cone. Also, Fig. 9 b) shows a significant gain increase of the double pitch helical antenna with truncated cone reflector in comparison with the standard one around 2.4 GHz, but the bandwidth of such an antenna gain is not increased.

2.4 Backfire monofilar helical antenna

This chapter gives the information about the effect of the ground plane size on the helical antenna radiation characteristics. It is found that as the diameter of the reflector decreases, the backfire radiation occurs and at the ground plane diameter smaller than the helix diameter it becomes dominant (Nakano et al., 1988). The analysis of a monofilar backfire helix was carried out through the example from chapter 2.1: $\lambda = 12.34$ cm, $\psi = 14^\circ$, $N = 12$, $r_w = 0.008\lambda$ and $D = 0.34\lambda$ with the reflector diameter of $d = 1.38\lambda$. This antenna can also be used in the form of monofilar backfire helix in the focus of a paraboloidal reflector. The results of simulations performed in FEKO show the radiation patterns and current distributions of the helical antennas with three different diameters of ground plane $d_1 = 0.7\lambda$, $d_2 = 0.35\lambda$ and $d_3 = 0.3\lambda$. In Fig. 10 a) helical antenna operates in standard axial mode where radiation is in forward direction where relative phase velocity $p = v/c$ satisfies the in-phase Hansen-Woodyard condition and the current distribution shows that surface wave is formed after the first minimum. There are no great discrepancies between this antenna and the one with larger reflector, as expected. As the diameter of the reflector decreases below 0.5λ , the decaying region of current distribution (Fig. 10) slightly shifts toward the end and becomes comparable to the surface region of the current. Also the amplitude of current in surface wave region decreases meaning that the backward radiation becomes larger. The antenna in Fig. 10 c) is the typical backfire monofilar helical antenna with the current distribution consisted only of a decaying current and a relative phase velocity nearly equal to one. It can be noticed that the forward and backward wave helical antennas achieve good but opposite sense circular polarization (Nakano et al., 1988).



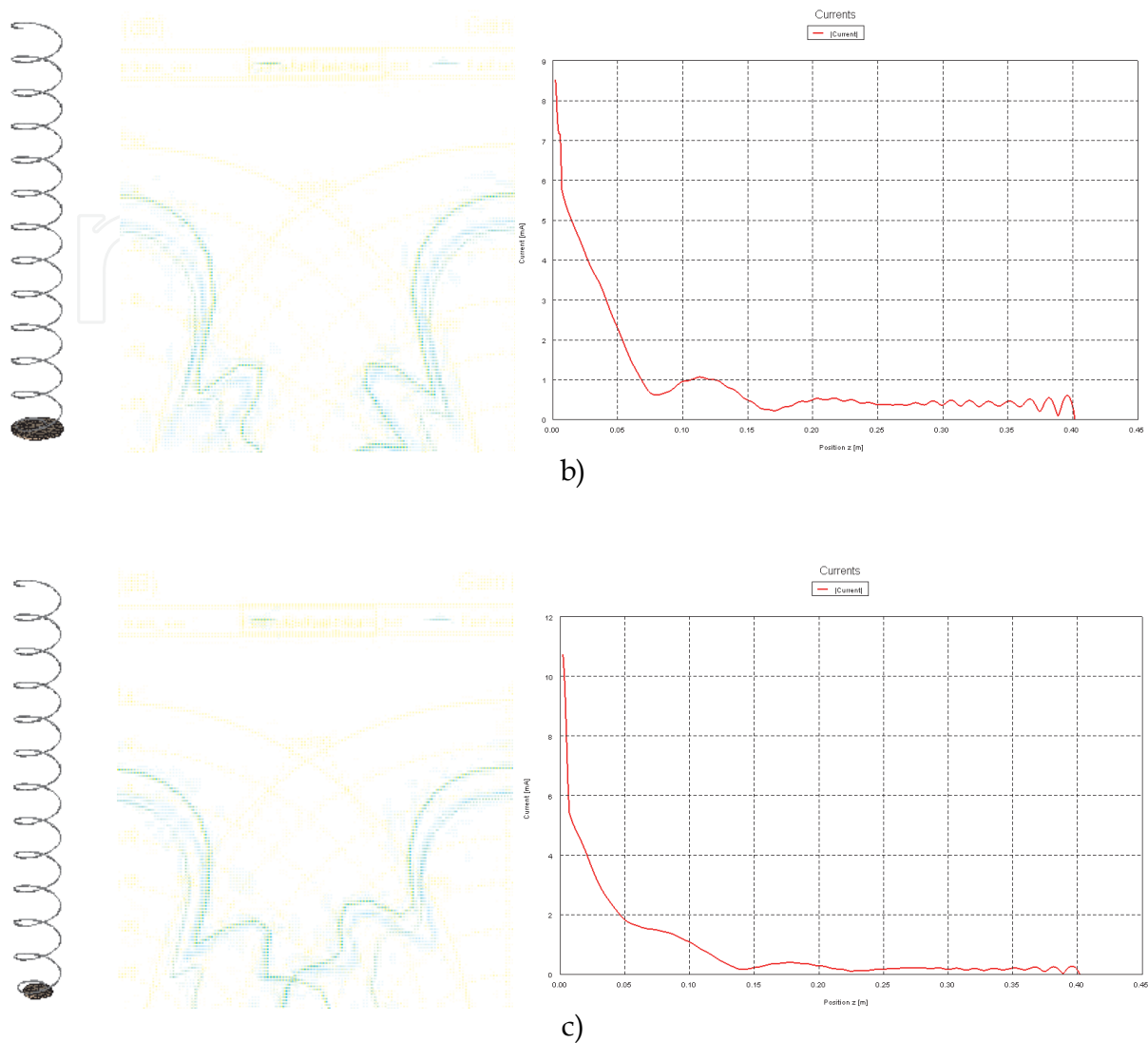


Fig. 10. The geometry, radiation pattern and current distribution of helical antenna with reflector of the diameter of a) $d_1 = 0.7\lambda$, b) $d_2 = 0.35\lambda$, and c) $d_3 = 0.3\lambda$.

3. Multifilar helical antennas

Beside the parameter modifications of monofilar helical antenna, the multiple number of wires in helix structure also offers interesting radiation performances for satellite communications. While monofilar helices are usually employed in transmission (Kraus, 1988), the multifilar helical antennas, bifilar and quadrifilar are mostly utilized at reception where wide beamwidth coverage is needed to track as many of the visible satellites as possible (Kilgus, 1974; Lan et al., 2004).

3.1 The bifilar helical antenna

Patton was the first to describe bifilar helical antenna (BHA) with backfire radiation achieving maximum directivity just above the cut-off frequency of the main mode of the

helical waveguide. The beamwidth broadens with frequency and for pitch angles of about forty five degrees, the beam splits and turns into a scanning mode toward broadside direction. As opposed to monofilar helical antenna, the backfire BHA radiates toward the feed point, its gain is independent of length (provided that the length is large enough) and the beamwidth increases with frequency (Patton, 1962).

Backfire bifilar helix is often used as a feed antenna because of its high efficiency, circularly polarized backward wave and low aperture blockage. In mobile handsets and various aerodynamic surfaces requiring low profile antennas side fed bifilar helical antenna can be used which produces a slant 45° linearly polarized omnidirectional toroidal pattern providing higher diversity gain in all directions (Amin et al., 2007).

In order for the bifilar helix to operate as backfire antenna, it is necessary that the currents flowing from the terminals to the ends of two helices are out of phase and the currents in the reversed direction are in phase. Hence, no radiation in forward direction is possible. This could be explained by the nature of the backward wave of current, where the phase is progressing toward the feed and the group velocity must be away from the feed point. A ground plane is not necessary in bifilar helical antenna design but this antenna usually achieves poor front-to-back (F/B) ratio which can cause interference problems when used as a receiving antenna. However, bifilar helical antenna with tapered feed end improves F/B ratio as well as the antenna power gain and axial ratio in comparison with conical and standard bifilar helical antenna (Yamauchi et al., 1981).

The BHA simulations are carried out in FEKO software on the basis of the following parameters (Yamauchi et al., 1981); the wavelength $\lambda = 10$ cm, circumference of the helical cylinder $C = \lambda$, the pitch angle $\psi = 12.5^\circ$, wire radius $r = 0.005\lambda$, tapering cone angle $\theta = 12.5^\circ$ and the number of turns in tapered section $n_t = 2.3$ and in uniform section $n_u = 3$. Three types of BHA with the same axial length were simulated: standard, conical and tapered BHA, Fig. 11 a). Tapered BHA is consisted of two sections of equal axial lengths, one corresponding to the first half of the conical BHA and the other to the half of the standard BHA. According to the radiation patterns in Fig. 11 b) and the results given in the Table 1, the tapered BHA provides the best performance of the BHA considering the F/B ratio and gain with satisfying axial ratio and decreased HPBW. It is important to note that the conical and tapered BHA's give better radiation characteristics than the standard BHA. Further investigation of the tapered BHA in terms of height reduction concerning the growing need for antenna miniaturization, shows that good BHA performance can be achieved with even smaller tapered bifilar helical antenna. The height of this antenna was reduced with a step of one spacing of the standard BHA ($p = C \tan \psi$) and the results are summarized in Table 2. The simulations obtained for the reduced version of tapered BHA yielded the best results for the one with $n_u = 1$ and $n_t = 2.3$ which corresponds to $2/3$ of the total length of the original BHA, with the geometry and radiation pattern shown in Fig. 12.

In order to reduce the antenna length, Nakano et al. examined bifilar scanning helical antenna with large pitch angle terminated with a resistive load. This antenna generates circularly polarized scanning radiation pattern from backfire to normal. The simulations show the scanning radiation patterns of the bifilar helix with six turns, pitch angle of 68° and diameter of 1.6 cm, through the frequency band from 1.3 - 2.5 GHz (Nakano et. al, 1991). Fig. 13 illustrates typical radiation patterns, the backfire conical and normal radiation pattern reaching the antenna gain of 10 dB, Fig. 13 a) and b), respectively.

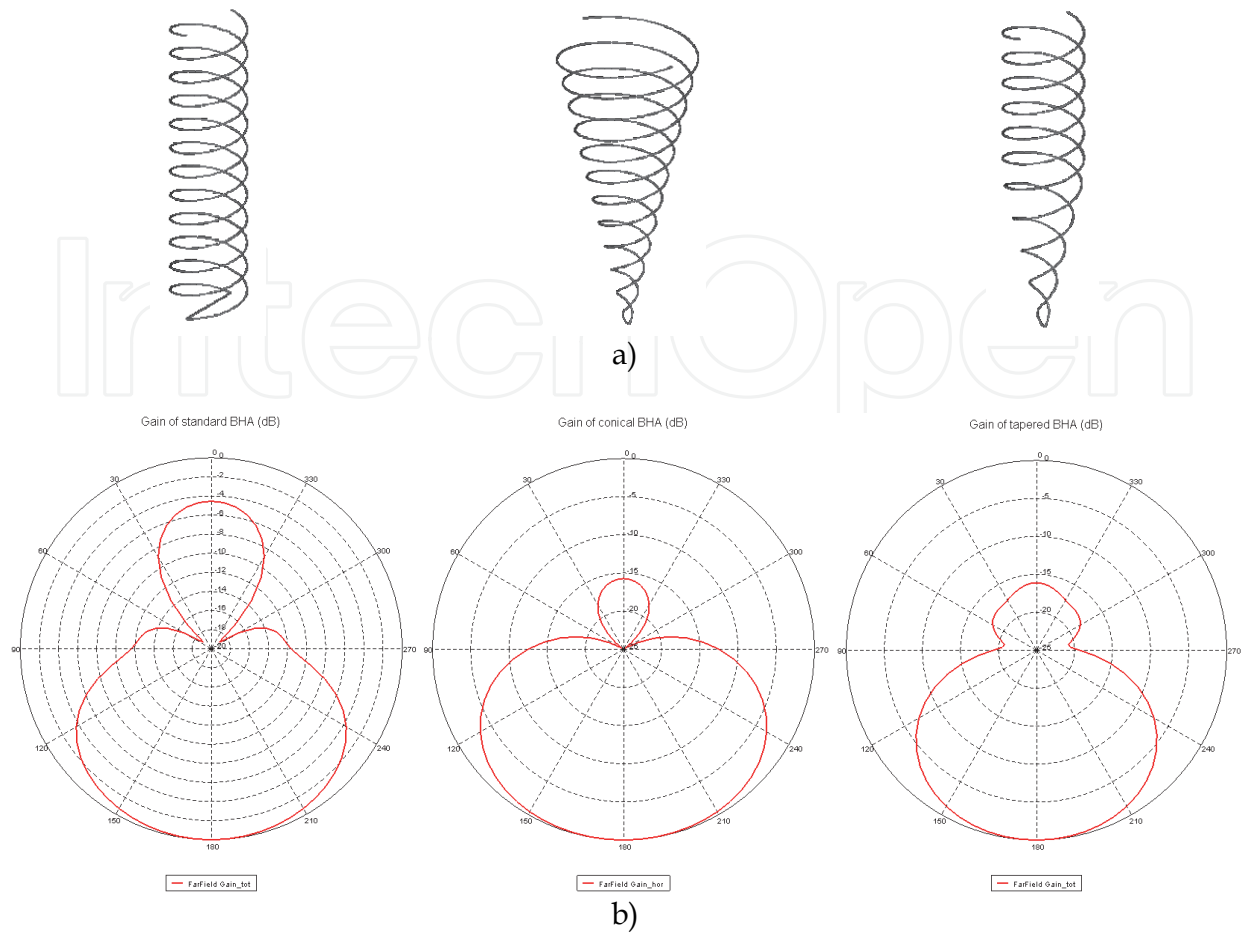


Fig. 11. a) Standard, conical and tapered BHAs, and b) their radiation patterns.

	F/B (dB)	Gain (dB)	AR	HPBW (°)
Standard BHA	4.5	5.6	0.79	111
Conical BHA	15.6	6.5	0.92	113
Tapered BHA	16	7.6	0.76	87

Table 1. Simulation results of radiation characteristics of standard, conical and tapered BHA.

	F/B (dB)	Gain (dB)	AR	HPBW (°)
Tapered BHA ($n_t = 1.5, n_u = 3$)	15.4	7.1	0.72	90
Tapered BHA ($n_t = 0.8, n_u = 3$)	11.2	5.7	0.89	120
Tapered BHA ($n_u = 0, n_t = 2.3$)	7.5	6	0.72	85
Tapered BHA ($n_u = 1, n_t = 2.3$)	14.8	7.8	0.65	82
Tapered BHA ($n_u = 2, n_t = 2.3$)	14.0	7.8	0.75	87

Table 2. Simulation results of reduced size tapered BHA.

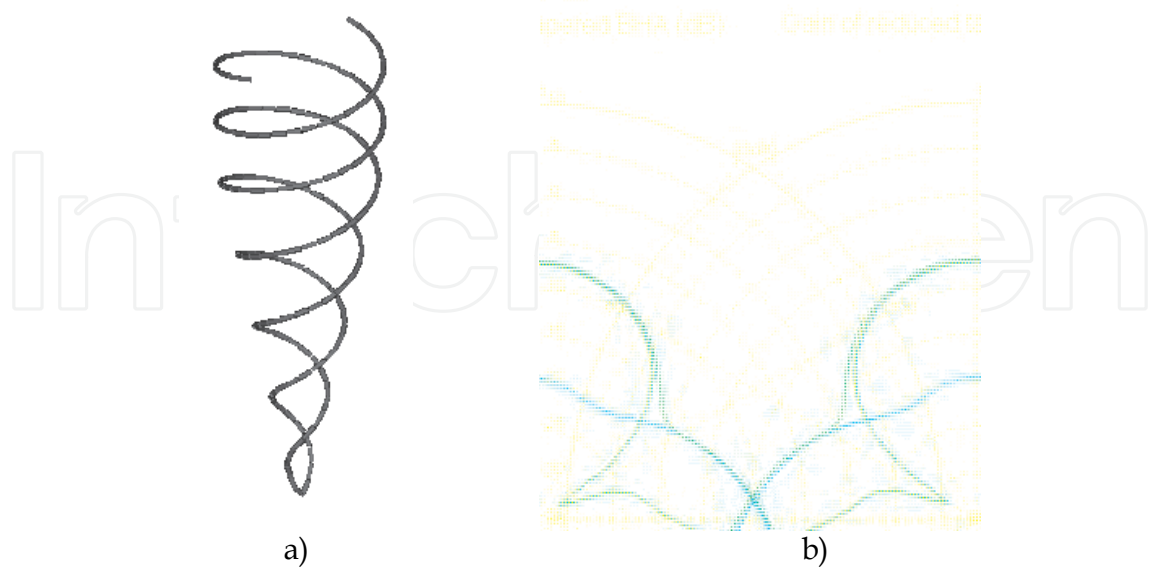


Fig. 12. Geometry and radiation patterns of reduced size BHA, a) and b) respectively.



Fig. 13. Typical radiation patterns of bifilar scanning helical antenna, a) conical at 1.6 GHz and b) normal radiation pattern at 2.1 GHz.

Contrary to monofilar helical antenna, the bifilar helical antenna yields scanning radiation mode when relative phase velocity $p = v/c = 1.0$. This is confirmed with the comparison of the simulated results with the experimental and calculated results (Nakano et al., 1991; Zimmerman, 2000) of the lobe direction for the different values of phase velocity, Fig. 14.

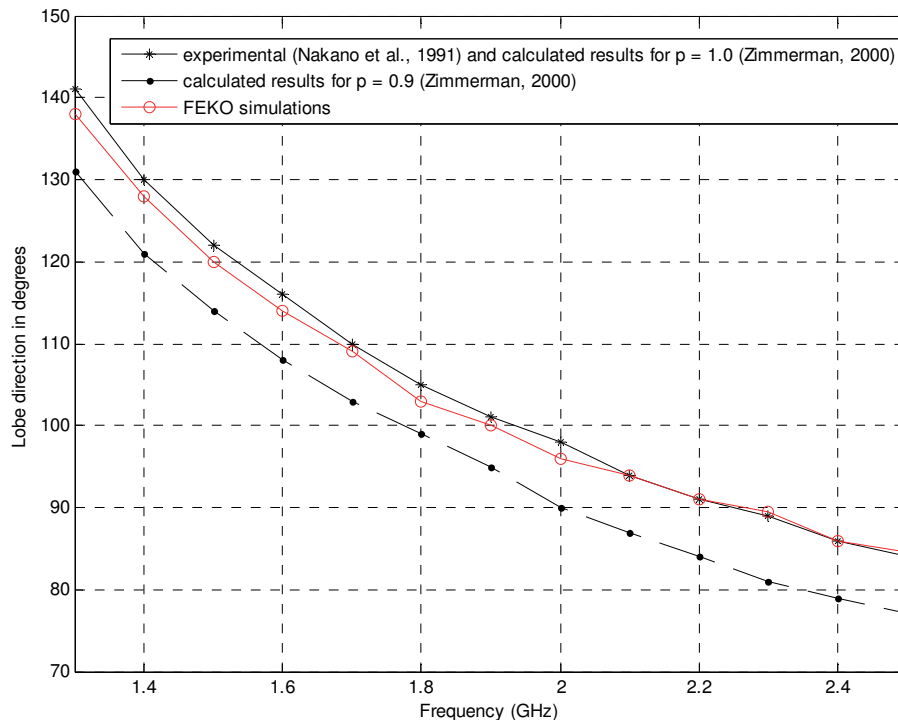


Fig. 14. The comparison of the simulated, calculated and experimental results for the lobe direction vs. frequency.

3.2 The quadrifilar helical antenna

The quadrifilar helical antenna (QHA), also known as the Kilgus coil, is mostly used for telemetry, tracking and command (TT&C) satellite systems due to its simplicity, small size, wide circularly polarized beam and insensitivity to nearby metal objects. The QHA consists of four helical wires equally spaced circumferentially and fed from the top or the bottom. The open ended QHA generally uses the length of each wire of $\lambda/4$ or $3\lambda/4$ with typical input impedance in the range 10 to 20 ohms while the short-circuited QHA uses $\lambda/2$ or λ length of each wire which produces resonant input impedance of nearly 50 ohms. Printed QHAs, convenient for high frequency applications, are manufactured using the dielectric substrate (Chew et al., 2002; Hanane et al., 2007) while wire QHA-s can be implemented on cylindrical, conical, square and spherical dielectric mechanical supports (Casey & Bansal, 2002; Hui et al., 2001). The size reduction of quadrifilar helical antennas can be achieved with geometrical reduction techniques such as sinusoidal (Fonseca et al., 2009; Takacs et al., 2010), rectangular (Ibambe et al., 2007), meander line (Chew et al., 2002) and other techniques (Letestu et al., 2006).

Radiation pattern of fractional turn resonant QHA is cardioid-shaped and circularly polarized with wide beamwidth, but by extending the fractional-turn QHA to an integral number of turns shaped-conical radiation pattern can be obtained for many applications in spacecraft communications (Kilgus, 1975).

The Kilgus coil consisted of four wires $\lambda/2$ long and forming a $1/2$ turn of a helix, generates a cardioid-shaped backfire radiation pattern with circular polarization and a very high HPBW

when two pairs are fed in phase quadrature and lower ends are short-circuited (Kilgus, 1968, 1974). The antenna is fed with a split sheath balun and the phase quadrature is achieved by adjusting the lengths of the wires.

The performance of the QHA is described with the following parameters: the length of one element consisted of two radials and a helical section l_{el} (integer number of $\lambda/2$), axial length between the radials l_{ax} and the number of turns N . We designed a half turn QHA for GPS L2 signal with the central frequency of $f = 1220$ MHz and the following parameters: $l_{el} = \lambda/2$, wire diameter $d = 2$ mm, bending radius $b_r = 5$ mm and width-to-height ratio $w/h = 0.44$ (the length of wires was adjusted to achieve phase quadrature so width w is the longitudinal width and h is axial height (l_{ax}) of the antenna). This is the so called self-phased QHA where the wire of one bifilar helix is longer than the resonant length, so that the current has a phase lead of 45° and the other is shorter in order to achieve a phase lag of 45° . Instead of infinite balun, we proposed a stripline structure for impedance matching and the support for helical wire. Fig. 15 c) shows that matching stripline is made of shorter part designed to counteract the imaginary part of the antenna input impedance and longer quarterwave part which is used to tune the real component of antenna input impedance to 50- Ω coaxial line impedance (Sekelja et al., 2009).

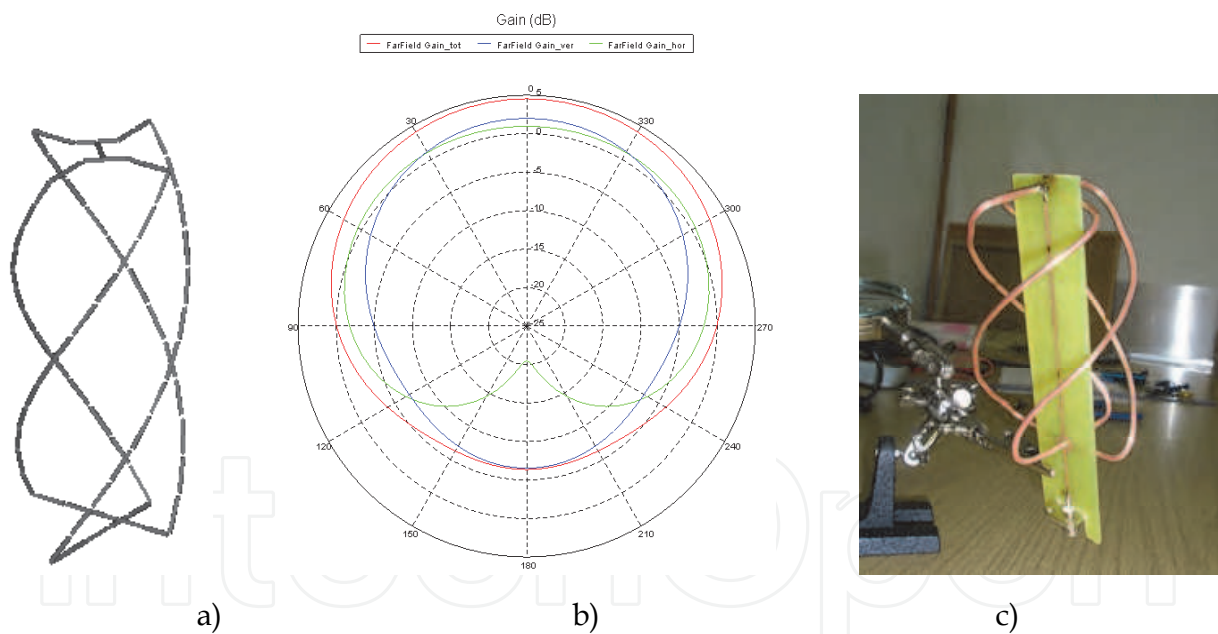


Fig. 15. The geometry with wire segments a) and simulated radiation patterns b) of QHA and c) the antenna prototype with stripline feeding structure.

In many satellite applications, it is also desirable to concentrate the radiated energy into a shaped conical beam with full cone angles from 120° to 180° (Kilgus, 1975). So, for the same frequency, $f = 1220$ MHz, we simulated a three turn QHA (Fig. 16 a)) fed in phase quadrature with short circuited ends which achieves gain decreasing from the maximum of 5.6 dB at the edge of the cone to the local minimum of -2.5 dB at the centre. Radiation pattern in Fig. 16 b) also shows that this antenna gives an excellent axial ratio.

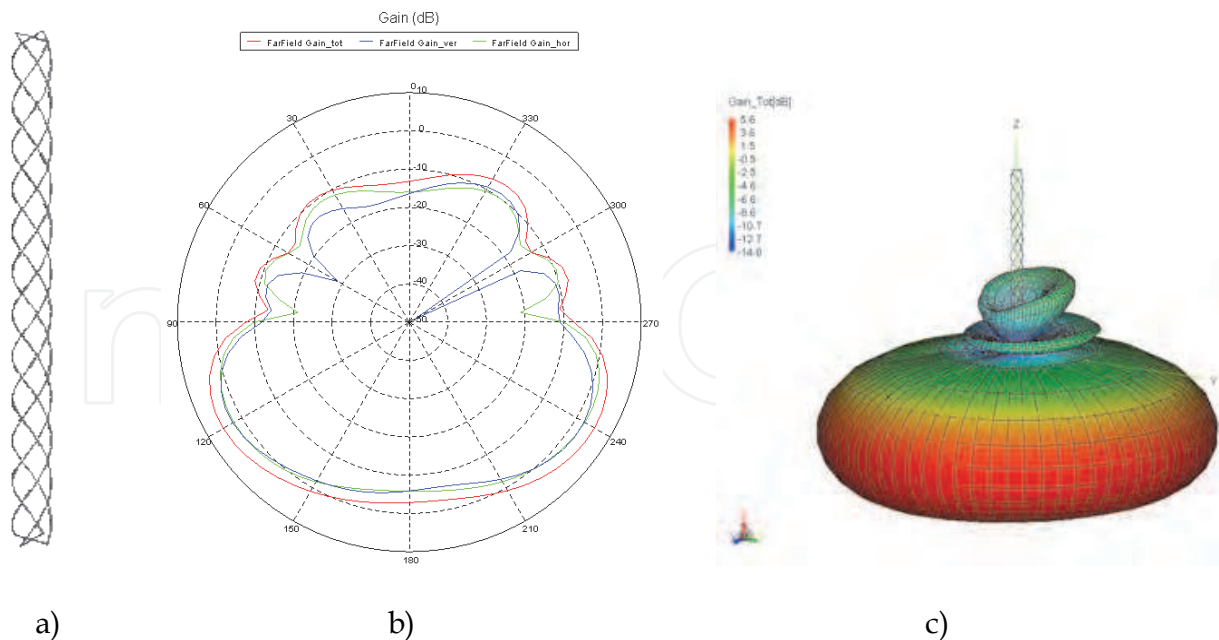


Fig. 16. a) The geometry, b) the 2D and c) 3D simulated radiation patterns of three turn QHA.

5. Conclusion

In this chapter, the basic theory and simulations of helical antennas are presented. It is shown that various radiation patterns can be obtained with conventional helical antenna and its modifications: forward and backward radiation, beam, normal and scanning radiation, from hemispherical to conical-shaped radiation patterns. The circular polarization is easily achieved (except for the normal mode) and it can be improved by end tapering. These modifications include the change of helix geometry, the size and shape of reflector, the number of wires and implementing some guiding structure.

However, when implementing real materials in practical design, they must be evaluated for their influence on the overall antenna performance. Thus, while the depicted analytical approach offers a tool for the optimal design and basic analysis of the helical antenna, although not completely impossible, it becomes too complex to be implemented in final decision about the practical design. The performances of the designed antenna must therefore be tested by some numerical tool or by measurements.

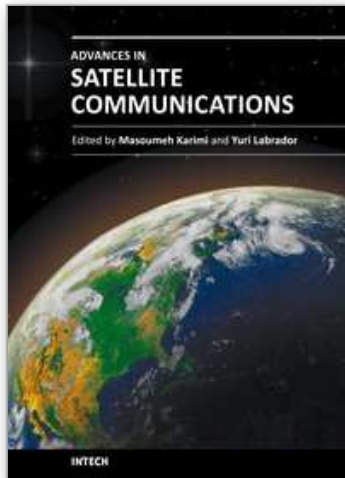
6. References

- Adekola, A. S., Mowete, A. I. & Ayorinde, A. A. (2009). Compact theory of the broadband elliptical helical antenna, *European Journal of Scientific research*, Vol. 31, No. 3, (2009), pp. 446-490, ISSN 1450-216X
- Amin, M., Cahill, R. & Fusco, V. Single feed low profile omnidirectional antenna with slant 45° linear polarization, *IEEE Transactions on Antennas and Propagation*, Vol. 55, No. 11, (November 2007), pp. 3087-3090, ISSN 0018-926X
- Barts, R. M. & Stutzman, W. L. (1997). A reduced size helical antenna, *Proceedings of IEEE Antennas and Propagation Society International Symposium*, ISBN 0-7803-4178-3, Montreal, Canada, July 1997.

- Blazevic, Z. & Skiljo, M. (2010). Bandwidth of the Helical Beam Antenna Loaded by a Dielectric Rod, *Proceedings of ICECom*, ISBN 978-1-61284-998-0, Dubrovnik, Croatia, September 2010.
- Bulgakov, B. M., Shestopalov, V. P., Shiskin, L. A. & Yakimenko, I. P. (1960). Symmetrical surface waves in a helix waveguide with a ferrite medium, *Journal of Radio and Electronic Physics*, Vol. 5, No. 11, (1960), pp. 102-119
- Carver, K. R. (1967). The helicone—a circularly polarized antenna with low side-lobe level, *Proceedings of the IEEE*, Vol. 55, No. 4, (April 1967), p. 559, ISSN 0018-9219
- Casey, J. P. & Basal, R. (1988). Dielectrically loaded wire antennas, *Proceedings of the IEEE*, Vol. 135, No. 2, (April 1988), pp. 103-110, ISSN 0950-107X
- Casey, J. P. & Basal, R. (1988) Square helical antenna with a dielectric core, *IEEE Transactions on Electromagnetic Compatibility*, Vol. 30, No. 4, (November 1988), pp. 429-436, ISSN 0018-9375
- Cha, A. G. (1972). Wave propagation on helical antennas, *IEEE Transactions on Antennas and Propagation*, Vol. 20, No. 5, (September 1972), pp. 556-560, ISSN 0018-926X
- Chew, D. K. C. & Saunders, S. R. (2002). Meander line technique for size reduction of quadrifilar helix antenna, *IEEE Antennas and Wireless Propagation Letters*, Vol. 1, No. 1, (2002.) pp. 109-111, ISSN 1536-1225
- Djordjevic, A. R., Zajic, A. G. & Ilic, M. M. (2006). Enhancing the gain of helical antennas by shaping the ground conductor, *IEEE Antennas and Wireless Propagation Letters*, Vol. 5, No. 1, (December 2006), pp. 138-140, ISSN 1536-1225
- Fonseca, N. J. G. & Aubert, H. (2009). Very compact quadrifilar helix antenna in VHF band with quasi hemispherical radiation pattern, *Proceedings of IEEE Antennas and Propagation Society International Symposium*, ISBN 978-1-4244-3647-7, Charleston, South Carolina, June 2009.
- Hanane, L., Hebib, S., Aubert, H. & Fonseca, N. J. G. (2007). Compact printed quadrifilar helix antennas for stratospheric balloons telemetry, *Proceedings of IEEE Antennas and Propagation Society International Symposium*, ISBN 978-1-4244-0877-1, Honolulu, Hawaii, June 2007.
- Hui, H. T., Yung, E. K. N. & Leung, K. W. (1997). Numerical and experimental studies of a helical antenna loaded by a dielectric resonator, *Radio Science*, Vol. 32, No. 2, (March-April 1997), pp. 295-304, ISSN 0048-6604
- Hui, H. T., Chan, K. Y. & Yung, E. K. N. (2001). The input impedance and the antenna gain of the spherical helical antenna, *IEEE Transactions on Antennas and Propagation*, Vol. 49, No. 8, (August 2001), pp. 1235-1237, ISSN 0018-926X
- Ibambe, M. G., Letestu, Y. & Sharaiha, A. (2007). Compact printed quadrifilar helical antenna. *Electronic Letters*, Vol. 43, No. 13, (June 2007), pp. 697-698, ISSN 0013-5194
- Kilgus, C. (1968). Multielement, Fractional Turn Helices. *IEEE Transactions on Antennas and Propagation*, Vol.16, No.4, (July 1968), pp. 499-500, ISSN 0018-926X
- Kilgus, C. (1974). Spacecraft and Ground Station Applications of the Resonant Quadrifilar Helix, *Proceedings of IEEE Antennas and Propagation Society International Symposium*, Vol.12, pp. 75-77, June 1974.
- Kilgus, C. (1975). Shaped-Conical Radiation Pattern Performance of the Backfire Quadrifilar Helix. *IEEE Transactions on Antennas and Propagation*, Vol. 23, No. 3, (May 1975), pp. 392-397, ISSN 0018-926X

- Klock, P. (1963). A study of wave propagation of helices, University of Illinois Antenna Laboratory Technical Report No. 68, March 1963.
- Kraft, U. R. & Mönich, G. (1990). Main-beam polarization properties of modified helical antennas, *IEEE Transactions on Antennas and Propagation*, Vol. 38, No. 5, (May 1990), pp. 589-597, ISSN 0950-107X
- Kraus, J. D. & Williamson J. C. (1948). Characteristic of helical antennas radiating in the axial mode, *Journal of Applied Physics*, Vol. 19, No. 1, (January 1948), pp. 87-96, ISSN 0021-8979
- Kraus, J. D. (1949). The helical antenna, *Proceedings of IRE*, Vol. 37, No. 3, (March 1949), pp. 263-272, ISSN 0096-8390
- Kraus, J. D. (1988). *Antennas* (2nd ed), McGraw-Hill Companies, ISBN 978-0070354227, New Delhi, India
- Lan, C. W., Chang, T. H. & Kiang, J. F. (2004). Helical antenna for GPS applications, *Proceedings of IEEE Antennas and Propagation Society International Symposium*, ISBN 0-7803-8302-8, June 2004.
- Letestu, Y. & Sharaiha, A. (2006). Broadband folded printed quadrifilar helical antenna, *IEEE Transactions on Antennas and Propagation*, Vol. 54, No. 5, (May 2006), pp. 1600-1604, ISSN 0018-926X
- Maclean, T. S. M. & Kouyoumjian, R. G. (1959). The bandwidth of helical antennas, *IRE Transactions on Antennas and Propagation*, Vol. 7, No. 5, (December 1959), pp. 379-386, ISSN 0096-1973
- Marsh, J. (1950). Current distributions on helical antennas, Project Report No. 339-10, The Ohio State University Research Foundation, February 28, 1950.
- Mimaki, H. & Nakano, H. (1998). Double pitch helical antenna, *Proceedings of IEEE Antennas and Propagation Society International Symposium*, ISBN 0-7803-4478-2, Atlanta, Georgia, June 1998.
- Nakano, H., Samada, Y. & Yamauchi, J. (1986). Axial mode helical antenna, *IEEE Transactions on Antennas and Propagation*, Vol. AP-34. No. 9, (September 1986), pp. 1143-1148, ISSN 0018-926X
- Nakano, H., Yamauchi, J. & Mimaki, H. (1988). Backfire radiation of a monofilar helix with a small ground plane, *IEEE Transactions on Antennas and Propagation*, Vol. 36, No. 10, (October 1988.), pp. 1359-1364, ISSN 0018-926X
- Nakano, H., Takeda, H., Honma, T., Mimaki, H. & Yamauchi, J. (1991.). Extremely low-profile helix radiating a circularly polarized wave, *IEEE Transactions on Antennas and Propagation*, Vol. 39, No. 6, (June 1991), pp. 754-757, ISSN 0018-926X
- Nakano, H., Mimaki, H. & Yamauchi, J. (1991). Loaded bifilar helical antenna with small radius and large pitch angle, *Electronic Letters*, Vol. 27, No. 17, (August 1991), pp. 1568-1569, ISSN 0013-5194
- Neureuther, A. R., Clock, P. W. & Mittra, R. (1967). A study of the sheath helix with a conducting core and its application to the helical antenna, *IEEE Transactions on Antennas and Propagation*, Vol. AP-15, No. 2, (March 1967), pp. 203-210, ISSN 0018-926X
- Olcan, D. I., Zajic, A. R., Ilic, M. M. & Djordjevic, A.R. (2006). On the optimal dimensions of helical antenna with truncated-cone reflector, *Proceedings of EuCAP*, ISBN 978-92-9092-937-6, Nice, France, November 2006.

- Patton, W. T. (1962). The backfire bifilar helical antenna, Technical Report No. 61, Electrical Engineering Research Laboratory, University of Illinois, September 1962.
- Sekelja, M., Jurica, J. & Blazevic, Z. (2009). Designing and testing the quadrafilar helical antenna, *Proceedings of SoftCOM*, ISBN 978-1-4244-4973-6, Hvar, Croatia, September 2009.
- Skiljo, M., Blazevic, Z., Jurisic, A. and Pandzic, K. (2010). Improving the Helical Antenna Performance by Changing the Pitch Angle and the Shape of Reflector, *Proceedings of SoftCOM*, ISBN 978-1-4244-4973-6, Bol, Croatia, September 2010.
- Sensiper, S. (1951). Electromagnetic wave propagation on helical conductors, Technical Report No. 194, MIT Research Laboratory of Electronic, May 16, 1951.
- Sensiper, S. (1955). Electromagnetic wave propagation on helical structures, *Proceedings of IRE*, ISSN 0096-8390, February 1955.
- Shestopalov, V. P., Bulgakov, A. A. & Bulgakov, B. M. (1961). Theoretical and experimental studies of helical dielectric antennas, *Journal of Radio and Electronic Physics*, Vol. 6, July 1961, pp. 1011-1019.
- Sultan, N., Moody, M., Whelpton, J. & Hodgson, C. (1984). Novel broadband double pitch cylindrical helical antenna for satellite and ground applications, *Proceedings of IEEE Antennas and Propagation Society International Symposium*, Vol.22, pp. 162-165, June 1984.
- Takacs, A., Fonseca, N. J. G. & Aubert, H. (2010). Height reduction of the axial-mode open-ended quadrifilar helical antenna, *IEEE Antennas and Wireless Propagation Letters*, Vol.9, (September 2010.) pp. 942-945, ISSN 1536-1225
- Vaughan, R. G. & Andersen, J. B. (1985). Polarization properties of the axial mode helix antenna, *IEEE Transactions on Antennas and Propagation*, Vol 33, No. 1, (January 1985), pp. 10-20, ISSN 0018-926X
- Wong, J. L. & King, H. E. (1979). Broadband quasi-taper helical antennas, *IEEE Transactions on Antennas and Propagation*, Vol. 27, No. 1, (January 1979), pp. 72-78, ISSN 0018-926X
- Wong, J. L. & King, H. E. (1982). Empirical Helix Antenna Design, *Proceedings of IEEE International Symposium on Antennas and Propagation*, p.p. 366-369, May 1982.
- Yamauchi, J., Nakano, H. & Mimaki, H. (1981). Backfire bifilar helical antenna with tapered feed end, *Proceedings of IEEE Antennas and Propagation Society International Symposium*, Vol. 19, pp. 683-686, June 1981.
- Zimmerman, R. K., Jr. (2000). Traveling wave analysis of a bifilar scanning helical antenna, *IEEE Transactions on Antennas and Propagation*, Vol 48, No. 6, (June 2000), pp. 1007-1009, ISSN 0018-926X



Advances in Satellite Communications

Edited by Dr. Masoumeh Karimi

ISBN 978-953-307-562-4

Hard cover, 194 pages

Publisher InTech

Published online 27, July, 2011

Published in print edition July, 2011

Satellite communication systems are now a major part of most telecommunications networks as well as our everyday lives through mobile personal communication systems and broadcast television. A sound understanding of such systems is therefore important for a wide range of system designers, engineers and users. This book provides a comprehensive review of some applications that have driven this growth. It analyzes various aspects of Satellite Communications from Antenna design, Real Time applications, Quality of Service (QoS), Atmospheric effects, Hybrid Satellite-Terrestrial Networks, Sensor Networks and High Capacity Satellite Links. It is the desire of the authors that the topics selected for the book can give the reader an overview of the current trends in Satellite Systems, and also an in depth analysis of the technical aspects of each one of them.

How to reference

In order to correctly reference this scholarly work, feel free to copy and paste the following:

Zoran Blazevic and Maja Skiljo (2011). Helical Antennas in Satellite Radio Channel, Advances in Satellite Communications, Dr. Masoumeh Karimi (Ed.), ISBN: 978-953-307-562-4, InTech, Available from: <http://www.intechopen.com/books/advances-in-satellite-communications/helical-antennas-in-satellite-radio-channel>

INTECH
open science | open minds

InTech Europe

University Campus STeP Ri
Slavka Krautzeka 83/A
51000 Rijeka, Croatia
Phone: +385 (51) 770 447
Fax: +385 (51) 686 166
www.intechopen.com

InTech China

Unit 405, Office Block, Hotel Equatorial Shanghai
No.65, Yan An Road (West), Shanghai, 200040, China
中国上海市延安西路65号上海国际贵都大饭店办公楼405单元
Phone: +86-21-62489820
Fax: +86-21-62489821

© 2011 The Author(s). Licensee IntechOpen. This chapter is distributed under the terms of the [Creative Commons Attribution-NonCommercial-ShareAlike-3.0 License](#), which permits use, distribution and reproduction for non-commercial purposes, provided the original is properly cited and derivative works building on this content are distributed under the same license.

IntechOpen

IntechOpen